Robust Feedback Control of Combustion Instability with Modeling Uncertainty

BOE-SHONG HONG, VIGOR YANG,* and ASOK RAY

Department of Mechanical Engineering, The Pennsylvania State University, University Park, Pennsylvania 16802

This paper presents the design of a robust feedback controller for suppressing combustion instabilities in propulsion systems with distributed actuators. The control synthesis procedure is based on the H_∞-optimization, which guarantees robust stability and performance within specified uncertainty bounds by taking into account the effects of unmodeled dynamics, sensor noise, and parametric errors. It makes use of an observer structure for robust estimation of combustion dynamics, and an H_∞ loop-shaping for performance requirements. Results of simulation experiments are presented to show how longitudinal pressure oscillations can be suppressed in a generic combustion chamber. The closed-loop control system exhibits robust stability and performance in the presence of exogenous disturbances and parametric errors.   © 1999 by The Combustion Institute

NOMENCLATURE

A	System parameter of generalized plant
A_p	System parameter of nominal plant
$\bar{a}$	Speed of sound in mixture
b_k	Spatial distribution of burning of control fuel at kth location
$\bar{C}_v$	Constant-volume specific heat for two-phase mixture
D_{ni}	Linear parameters, Eq. (12)
$\mathbf{d}$	Plant disturbance
E_{ni}	Linear parameters, Eq. (12)
e	Internal energy
ΔH_c	Heat of combustion of control fuel
h	Source term in wave equation
I	Identity matrix
J	Cost functional
K	Dynamics of robust controller
L	Length of combustor
$\dot{m}_{in}$	Mass flow rate of control fuel
P	Dynamics of generalized plant
p	Pressure
Q	Rate of energy release in gas phase
$\mathbf{q}$	Conductive heat flux
q	Weighting factor of plant dynamics
$\bar{R}$	Gas constant for two-phase mixture
r	Weighting factor of control action
$\mathbf{r}$	Position vector
s	Independently complex variable in frequency domain
T	Temperature
t	Time
u	Control output of secondary-fuel injector
V	Volume of combustion chamber
$\boldsymbol{\nu}$	Input vector associated with distributed control source
U_n	Control input of nth mode
$\mathbf{v}_g$	Velocity of gas phase
W_d	Shaping filter associated with plant disturbance
W_p	Performance weighting function associated with pressure response
W_u	Performance weighting function associated with control fuel
W_τ	Stability weighting function associated with time-delay errors
W_θ	Shaping filter associated with sensor noise
$\mathbf{w}$	Generic disturbance; $\mathbf{w} = [\mathbf{w}_s^T \; \mathbf{w}_d^T \; \mathbf{w}_\theta^T \; w_\tau]^T$
$\mathbf{w}_d$	Weighted plant disturbance
$\mathbf{w}_s$	Disturbance induced from plant uncertainty
w_τ	Disturbance induced from model error of time-delay function
$\mathbf{w}_\theta$	Weighted sensor noise
$\dot{w}_c$	Burning rate of control fuel
$\mathbf{x}$	State vector of generalized plant
$\mathbf{x}_p$	State vector of nominal plant
$\mathbf{y}$	Sensor output vector
$\mathbf{z}$	Objective variable; $\mathbf{z} = [\mathbf{z}_s^T \; \mathbf{z}_p^T \; z_u \; z_\tau]^T$
$\mathbf{z}_s$	Stability variable associated with plant uncertainty
$\mathbf{z}_u$	Performance variable associated with control fuel

───────────

*Corresponding author. E-mail: vigor@psu.edu.

$\mathbf{z}_p$ Performance variable associated with pressure response

z_τ Stability variable associated with time-delay errors

Greek Symbols

ρ Density of two-phase mixture

φ_n Normal mode function of nth mode

$\boldsymbol{\eta}$ Amplitudes of mode shapes

η_n Time-varying amplitude of nth mode

Δ Uncertainty operator of robust performance

Δ_p Plant model uncertainty

Δ_τ Phase uncertainty induced from time-delay errors

δp Uncertainty bound of plant model

$\delta \tau$ Uncertainty bound of time delay

$\bar{\gamma}$ Specific heat ratio for mixture

θ Sensor noise

ω_n Normal frequency of nth mode

τ_k Time delay of kth combustion control source

$\boldsymbol{\tau}_v$ Viscous stress tensor

Superscripts

$\cdot$ Time derivative

$^-$ Mean quantity

NL Nonlinear term

$'$ Fluctuation

T Transpose

Subscripts

c Control input

g Gas phase

ℓ liquid phase

INTRODUCTION

The use of feedback control techniques to modulate combustion processes in propulsion systems has recently received extensive attention [1–3]. Most of the previous studies involve direct implementation of control techniques originally designed for mechanical devices, and very limited efforts have so far been devoted to the treatment of uncertainties due to unmodeled dynamics and parametric errors. It is well established that the intrinsic coupling between flow oscillations and transient combustion re-

sponses prohibits detailed and precise modeling of the various phenomena in a combustion chamber. All the existing models are subject to uncertain dynamics and parametric errors resulting from simplifying assumptions about the physical processes and the associated mathematical approximations. This paper presents a robust feedback controller for suppressing combustion instabilities in propulsion systems. Emphasis is laid on the treatment of model uncertainties, plant disturbances, and sensor noises for the tradeoff between robust stability and performance.

A variety of feedback-control techniques, summarized in Table I, have been used for suppressing combustion instabilities. The most primitive type is the proportional (P)-controller in a single-input and single-output (SISO) setting, in which stability and performance are achieved only by an operational amplifier between the sensor and actuator. The P-controller can be extended to form a proportional-integral-derivative (PID) control system, in which the I-control is used for achieving zero steady error, since it integrates the error in time, and the D-control serves to enhance the transient response, since it regulates the tendency of motion [4]. Conceptually, there are only three control parameters in a single PID controller module, so that the controller design is greatly simplified. However, for high-order plant dynamics, such a low-order controller may not satisfy various performance requirements. For linear systems, a PID controller can be extended to accommodate a filter with phase compensation in the frequency domain, or to form an integral state-feedback controller in the time domain. If all states cannot be measured, an observer is needed for output-feedback control [5, 6]. It is not difficult to design an observer for a finite-dimensional linear time-invariant (FDLTI) system, but it is much more challenging to design one for a time-varying or nonlinear system.

In the frequency domain, the open-loop dynamics of an FDLTI system can be conveniently represented by the Bode plot, through either physics-based modeling or system identification, or a combination of the two [1, 7–12]. The representation of system dynamics in the frequency domain simplifies the filter design, and the stability analysis can be based on the

TABLE 1

Survey of Active Combustion Control Techniques

Control Technique	Application	References	Remarks
PID design	nonlinear generic combustion instability	Fung and Yang [4]	1. Easy to adjust control parameters. 2. May not fulfill various performance requirements.
Bode-Nyquist frequency domain design and root locus	Generic combustion instability Low-frequency combustion instability Low-frequency combustion instability Coaxial dump combustor Longitudinal combustion instability in premixed combustor Thermoacoustic instability Liquid-fueled combustion systems	Bloxsidge et al. [7] Langhorne et al. [8] Fung et al. [1] Shadow et al. [9] Gulati and Mani [10] Annaswamy and Ghoniem [11] Hantschk et al. [12]	1. Easy to identify systems and design controller in frequency domain. 2. Fail in time-varying and nonlinear systems. 3. Only for SISO, can be more general in H_∞ and μ control. 4. Controllability and observability can not be predicted. 5. Easy for filter design. 6. Can serve as the basis of phase-lead and phase-lag compensator design.
Observer-based design: adaptive observer and model-based observer	Thermoacoustic instability in rocket motor Longitudinal combustion instability	Yang et al. [5] Neumeier and Zinn [6]	1. Nominal model-based observer can be extended to optimal LQG regulator. 2. Adaptive observer has no guarantee of convergence; its algorithm is one branch of the gradient iterative rules.
LQR and LQG control	Thermoacoustic instability in premixed laminar combustor	Annaswamy et al. [11]	1. LQR control has optimal and robust properties of gain and phase margins, but requires measurements of all states. 2. LQG control has no robust property and is used only for rejection of intensity-known noise.
LMS adaptive and neural network back propagation	Generic combustion instability Boiler combustion systems Dump combustor Large-scale solid rocket motor	Billoud et al. [18] Allen et al. [19] Kemal and Bowman [20] Koshigoe et al. [21]	1. Sensitive to initial conditions and gradient dynamic parameters. 2. Has similar algorithm in System ID. 3. May be replaced by off-line ID plus Bode-Nyquist or observer-based controller.
Fuzzy logic control	Longitudinal combustion instability	Menon and Sun [22]	1. Only effective when many states can be sensored. 2. Need experience to set up logic rules and scales. 3. Not used solo.
Lyapunov-based design	Generic combustion instability	Krstic [28]	1. Need more generalized control algorithms. 2. Nonlinear H_∞ control is based on Lyapunov design, but with general algorithms.

Nyquist criterion. The robustness of a controller is traditionally predicted in terms of phase and gain margins for single-input single-output (SISO) systems. When uncertainties are simultaneously present in both phase and gain, the issue of robustness can be expressed by the H_∞-based structured singular value (μ) of the closed-loop system [13–15].

Among the various time-domain tools for controller design, the linear quadratic regulator (LQR) controller appears to be the most robust, with its gain margin in the range of $[1/2, \infty)$ and at least $60°$ phase margin [16]. However, the LQR controller can be applied only if all the states can be measured without any appreciable noise contamination. Otherwise, a state estimator is needed to meet this requirement. The resulting output-feedback control system is known as the linear quadratic Guassian (LQG) controller, if a Kalman filter is used as the state estimator. The scheme may be further extended for nonlinear systems using an energy method in terms of the Lyapunov function. The major deficiency of the LQG technique lies in its failure to guarantee any gain and phase margin [17]. The H_∞-based structured singular value (μ) approach allows for quantification of robust stability and performance for bounded uncertainties [14].

Non-model-based controllers, such as least mean square (LMS) and artificial neural network back-propagation adaptive controllers, employ iterative approaches to update control parameters in real time [18–21]. However, those methods often encounter difficulties of numerical divergence and local optimization, and consequently may not guarantee stability and performance. In addition, most adaptive algorithms do not accommodate a physical model of plant dynamics. It is often risky to establish general rules for performance improvement and fault diagnostics based on approximate reasoning, such as fuzzy logic [22]. Moreover, formulation of fuzzy logic rules requires an extensive physical understanding and operations experience that is not usually available for combustion dynamics.

While the control schemes summarized in Table I have been employed in various combustion problems with some success, direct implementation of these techniques on practical propulsion systems may not be feasible, due to lack of robustness, reliability, and operationability. Compared with mechanical devices, a combustion chamber with feedback control of fuel burning exhibits several distinct features [1]:

- distributed actuation arising from the burning of injected fuel;

- time lag associated with the complex chain of fuel injection-atomization-ignition-combustion processes;
- intensive noise due to intrinsic fluid dynamic and combustion unsteadiness;
- time variation of mean flow conditions due to transient operation of the chamber; and
- model uncertainties and parametric errors resulting from physical assumptions and mathematical approximations employed for simulating system dynamics.

In view of the above, this paper uses the H_∞ theory [13] to design a robust feedback control scheme for suppression of combustion instabilities. The controller provides robust stability and performance relative to specified bounds of model uncertainties, parametric errors and exogenous disturbances (e.g., chamber perturbations and sensor noise). The control law can be extended over a wide range of operating conditions.

The outline of this paper is as follows. First, a theoretical model of unsteady motions in a combustion chamber with feedback control is formulated. The formulation is based on a generalized wave equation that accommodates the effects of acoustic waves and combustion dynamics. Control actions are achieved by injecting secondary fuel into the chamber according to the instantaneous flow conditions. Physically, the reaction of the injected fuel with the primary combustion flow produces a modulated distribution of external forcing to the oscillatory flow field, and can be conveniently modeled as an assembly of point actuators. After a procedure equivalent to the Galerkin method, the governing wave equation reduces to a system of ordinary differential equations with time-delayed inputs for the amplitude of each acoustic mode, serving as the basis for the controller design.

The second part of the work involves formulation of a robust feedback control law. The key issues in the control analysis and synthesis are: (i) treatment of parametric uncertainties, time delays, and unmodeled dynamics; and (ii) rejection of exogenous disturbances (e.g., chamber perturbations and sensor noise). A series of simulation experiments are conducted to examine the robust stability and performance of the
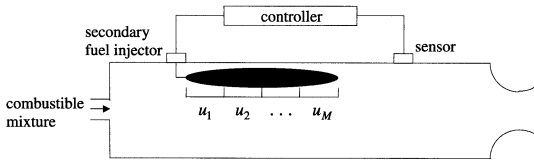
Fig. 1. Schematic Diagram of Feedback Control System with Distributed Actuators.

closed-loop control system. The relationships among the uncertainty bound of system dynamics, the response of flow oscillations, and the controller performance are investigated and quantified.

MODELING OF COMBUSTION DYNAMICS

The combustion system under consideration is shown schematically in Fig. 1, which represents a generic model for several types of air-breathing combustors, such as those used in ramjet and gas-turbine engines. Fuel and oxidizer are delivered to the combustion chamber, in which large excursions of unsteady motions take place due to the internal coupling between flow oscillations and transient response of combustion. The strategy described by Fung $et\ al$. [1] is followed for robust closed-loop control of combustion instabilities. First, the instantaneous chamber conditions are monitored by sensors at sufficiently high sampling rates to capture the transient characteristics of unsteady motions. The sensor signals are then processed by a controller to modulate the mass flow rate of a secondary supply of fuel. Finally, the injected fuel reacts with the combustor flow as it travels downstream, exerting a distribution of external influences on the oscillatory flowfield for instability control.

The formulation of combustion dynamics is constructed using the same approach as that employed in previous works on state-feedback control with distributed actuators [1, 4]. In essence, the medium in the combustion chamber is treated as a two-phase mixture. The gas phase contains inert species, reactants, and combustion products. The liquid phase is comprised of fuel and/or oxidizer droplets, and its unsteady behavior is modeled as a distribution of time-varying mass, momentum, and energy

perturbations to the gas-phase flowfield. If the droplets are taken to be dispersed, the conservation equations for a two-phase mixture is written in the following form, involving the mass-averaged properties of the flow:

$$\text{mass} \qquad \frac{\partial \rho}{\partial t} + \mathbf{v}_g \cdot \nabla \rho = W \qquad (1)$$

$$\text{momentum} \qquad \rho \frac{\partial \mathbf{v}_g}{\partial t} + \rho \mathbf{v}_g \cdot \nabla \mathbf{v}_g = -\nabla p + \boldsymbol{F} \qquad (2)$$

$$\text{energy} \qquad \frac{\partial p}{\partial t} + \bar{\gamma} p \nabla \cdot \mathbf{v}_g = -\mathbf{v}_g \cdot \nabla p + P \qquad (3)$$

where

$$W = -\rho \nabla \cdot \mathbf{v}_g - \nabla \cdot (\rho_\ell \delta \mathbf{v}_\ell) \qquad (4)$$

$$\boldsymbol{F} = \nabla \cdot \boldsymbol{\tau}_v + \delta \mathbf{F}_\ell + \delta \mathbf{v}_\ell \bar{\omega}_\ell \qquad (5)$$

$$P = (\bar{R}/\bar{C}_v)[Q + \delta Q_\ell + \nabla \cdot \mathbf{q} + \delta \mathbf{v}_\ell \cdot \mathbf{F}_\ell + \{(h_\ell \\ - e_g) + 1/2(\delta \mathbf{v}_\ell)^2\}\bar{\omega}_\ell - \bar{C}_v T_g \nabla \cdot (\rho_\ell \delta \mathbf{v}_\ell)] \qquad (6)$$

and $\delta \mathbf{v}_\ell = \mathbf{v}_\ell - \mathbf{v}_g$, $\delta h_\ell = h_\ell - C_\ell T$. The subscripts g and ℓ signify the mass-averaged quantities for the gas and liquid phases, respectively, and ρ is the density of the mixture. The viscous stress tensor and conductive heat flux vector are represented respectively by $\boldsymbol{\tau}_v$ and $\mathbf{q}$. The energy Q is released by homogeneous reactions in the gas phase. The force of interaction and energy transfer between gas and liquid are $\delta \mathbf{F}_\ell$ and δQ_ℓ, respectively.

Whatever physical means are devised, control inputs must be mathematically treated as forcing functions in the above conservation equations. Therefore, Eqs. (1)–(3) are modified by adding control inputs W_c, $\boldsymbol{F}_c$, and P_c on the right-hand sides. The subscript c represents the variables manipulated by the controller. The effects of heat release from the injected secondary fuel, P_c, takes the form

$$P_c = \frac{\bar{R}}{\bar{C}_v} Q_c = \frac{\bar{R}}{\bar{C}_v} \dot{w}_c \Delta H_c, \qquad (7)$$

where Q_c stands for the rate of energy release in the gas phase, $\dot{w}_c$ for the burning rate of the control fuel (mass/time-volume), and ΔH_c for the heat of combustion per unit fuel mass.
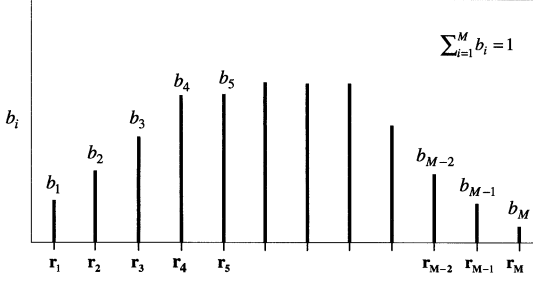
Fig. 2. Spatial Distribution of Actuator Output

A wave equation governing the unsteady motions is then derived by decomposition of all dependent variables as sums of the mean and fluctuation parts. Thus

$$\rho = \bar{\rho} + \rho'(\mathbf{r}, t); \ \mathbf{v}_g = \bar{\mathbf{v}}_g(\mathbf{r}) + \mathbf{v}'_g(\mathbf{r}, t);$$

$$p = \bar{p} + p'(\mathbf{r}, t) \tag{8}$$

Substituting Eq. (8) into Eqs. (1)–(3), collecting coefficients of like powers, and rearranging the results yields the following wave equation in terms of pressure fluctuation:

$$\nabla^2 p' - \frac{1}{\bar{a}^2} \frac{\partial^2 p'}{\partial t^2} = h + h_c \tag{9}$$

where h contains all physical processes of acoustic motion, mean flow, and combustion under conditions with no external forcing. The explicit expression is given by Fung [23].

The control source h_c arising from combustion of the injected fuel can be treated as a distributed actuator, with its spatial distribution approximated by an array of M discrete sources [1]. With the use of a generalized time-lag theory, the fuel control is expressed as:

$$h_c = -\frac{\bar{R}\Delta H_c}{\bar{a}^2 \bar{C}_v} \sum_{k=1}^{M} \frac{\partial \dot{m}_{in}(t - \tau_k)}{\partial t} b_k \delta(\mathbf{r} - \mathbf{r}_k) \tag{10}$$

where $\dot{m}_{in}$ stands for the mass flow rate of the injected fuel. The time delay, τ_k, is the time at which an element of fuel burns at the kth combustion source, measured from the instant of its injection. The spatial distribution parameter, b_k, shown in Fig. 2, measures the fraction of the control fuel currently burning within the volume represented by the kth combustion source, located at $\mathbf{r}_k$. Conservation of mass requires that $\sum_{k=1}^{M} b_k = 1$.

Since the source terms in the wave equation (9) and its associated boundary conditions are treated as small perturbations to the acoustic field, within second-order accuracy, the solution can legitimately be approximated by a synthesis of the normal modes of the chamber with time-varying amplitudes $\eta_n(t)$.

$$p'(\mathbf{r}, t) = \bar{p} \sum_{n=1}^{\infty} \eta_n(t)\varphi_n(\mathbf{r}) \tag{11}$$

where φ_n is the normal mode function. After substituting Eq. (11) into Eq. (9), and applying a spatial-averaging technique equivalent to the Galerkin method [24], the following system of equations is obtained for the temporal evolution of each mode.

$$\ddot{\eta}_n + \omega_n^2 \eta_n + \sum_{i=1}^{N} [D_{ni}\dot{\eta}_i + E_{ni}\eta_i]$$

$$+ F_n^{NL}(\eta_1, \eta_2, \cdots \dot{\eta}_1, \dot{\eta}_2 \cdots)$$

$$= U_n(t) + d_n(t), n = 1, 2, \cdots N \tag{12}$$

where $d_n(t)$ denotes plant disturbances. The coefficientsi D_{ni} and E_{ni} arise from linear processes and are modeled as frequency-dependent variables. The function F_n^{NL} represents all nonlinear effects of gasdynamic coupling and combustion response. The control input to the nth mode takes the form

$$U_n(t) = \frac{\bar{R}\Delta H_c}{\bar{C}_v \bar{p} V} \sum_{k=1}^{M} \frac{\partial \dot{m}_{in}(t - \tau_k)}{\partial t} b_k \varphi_n(\mathbf{r}_k) \tag{13}$$

The state of the acoustic field must be determined to complete the formulation. In the present study, the instantaneous pressure oscillation is monitored by a finite number of point sensors, located at positions $\mathbf{r}_{si}$. The output signal of each sensor becomes:

$$y_i(t) = \bar{p} \sum_{n=1}^{N} \eta_n(t)\varphi_n(\mathbf{r}_{si}) + \theta_i \tag{14}$$

where θ_i is the measurement noise with respect to the ith sensor.

The formulation described above provides a useful framework for treating feedback control of combustion instability. However, direct application of the model to practical problems must be performed with caution, because of the fol-

lowing uncertainties, which arise in the development of a robust control law.

- *Uncertainties in modeling combustion dynamics:* The intrinsic complexities in combustor flows prohibit precise estimation of system parameters, such as D_{ni} and E_{ni} in Eq. (12), and time delays τ_k's and spatial distribution b_k's in Eq. (13), without considerable errors. Furthermore, the model may not accommodate all the essential processes and involves uncertainties because of the physical assumptions and mathematical approximations employed.

- *Uncertainties in model reduction:* The finite-dimensional model in Eq. (12) is truncated from the infinite-dimensional wave equation. This truncated model is used for the controller design, and the dynamics of the unmodeled high-frequency modes are treated as part of model uncertainties.

- *Uncertainties in geometric-configuration and boundary-condition specifications:* The combustor geometry and boundary conditions determine the effectiveness of the truncated model for controller design. The difference between geometry of the real combustor and that of the model therefore is a source of uncertainties. In addition, variations in boundary conditions due to environmental changes cause additional uncertainties.

- *Uncertainties in operating conditions:* The model parameters depend on the mean-flow conditions that are determined by the operating range of the combustion chamber. An uncertainty is included in the model to take into account wide-range operations.

To facilitate the robust controller design, the above sources of uncertainties are lumped together into two full block uncertainties; one is associated with the combustion dynamics and the other with the distributed process of the control fuel. To this end, the plant dynamics equations (12)–(14) are modified to include uncertainties and are represented by the following state-space model:

$$\dot{\mathbf{x}}_p = (A_p + \Delta_p)\mathbf{x}_p + G_1\boldsymbol{\nu} + G_2\mathbf{d}$$
$$\mathbf{y} = C\mathbf{x}_p + \boldsymbol{\theta} \tag{15}$$

where $\mathbf{x}_p = (\xi^T \ \xi^T)^T$ with $\dot{\xi} = \boldsymbol{\eta}$, and $\boldsymbol{\eta} \equiv [\eta_1, \eta_2, \cdots, \eta_N]^T$. The nominal linear system matrices are:

$$A_p \equiv \begin{bmatrix} 0 & I \\ -\Omega - E & -D \end{bmatrix} \tag{16}$$

where $\Omega \equiv diag(\omega_1^2, \ \omega_2^2, \cdots, \omega_N^2)$

The input vector $\boldsymbol{\nu}(t)$ associated with a set of point actuation is related to the mass injection rate of the secondary fuel, $\dot{m}_{in}$, as

$$\boldsymbol{\nu}(t) = \begin{bmatrix} b_1\dot{m}_{in}(t - \tau_1 - \delta\tau_1) \\ b_2\dot{m}_{in}(t - \tau_2 - \delta\tau_2) \\ \vdots \\ b_M\dot{m}_{in}(t - \tau_M - \delta\tau_M) \end{bmatrix} \tag{17}$$

where $\delta\tau$ is the model error of the time-delay function. Equation (17) represents the actuator dynamics arising from the combustion of the injected control fuel, and its nominal transfer function is of the form:

$$A(s) = [b_1e^{-\tau_1 s} \ b_2e^{-\tau_2 s} \cdots b_Me^{-\tau_M s}]^T \tag{18}$$

The uncertainties associated with the spatial distribution b_i of the control source is not considered herein, for the sake of simplicity, but can be treated following the same procedure. The model and parametric uncertainties are represented by a differential operator Δ_p, and can be properly treated as disturbances of the plant, $\mathbf{w}_s(t) = \Delta_p(\mathbf{x}_p(t))$. The bound of the operator Δ_p is characterized by the induced L_2-gain (which is also the H_∞-gain for linear time-invariant systems) as:

$$\|\Delta_p\|_\infty < \delta p \tag{19}$$

Physically, the above equation implies that the dynamics of the uncertainty operator yields an energy-amplification relationship from its input $\mathbf{x}_p$ to output $\mathbf{w}_s$ as follows:

$$\int_0^T \|\mathbf{w}_s\|^2 \, dt < \int_0^T \delta p^2\|\mathbf{x}_p\|^2 \, dt \quad \forall \, T \in [0, \infty) \tag{20}$$

DESIGN OF ROBUST FEEDBACK CONTROLLER

This section describes how the stability and performance of a robust feedback controller can be achieved using the following two building blocks.
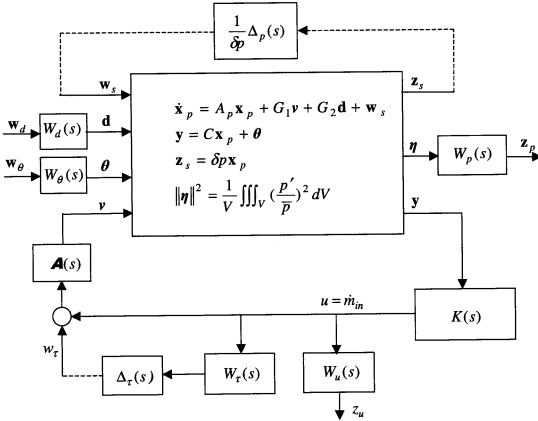
Fig. 3. Generalized Plant Model of Combustion Dynamics.

1. *Construction of a generalized plant model:* The generalized plant model $P(s)$ augments the nominal model of the plant dynamics by including model uncertainties and performance weights;
2. *Synthesis of an H_∞ controller:* A robust controller $K(s)$ is developed to guarantee stability and performance based on the generalized plant model.

Generalized Plant Model

Figures 3 and 4 show how the generalized plant model $P(s)$ interacts with the robust feedback controller $K(s)$ that processes the (pressure) sensor output **y** to generate the mass flow rate $\dot{m}_{in}$ of the injected control fuel. The major role of $K(s)$ is to regulate the energy amplification from the generic disturbance **w** to the objective variable **z**. Note that **w** consists of disturbances induced by plant uncertainties $\mathbf{w}_s$ and modeling errors of the time delay function w_τ, weighted
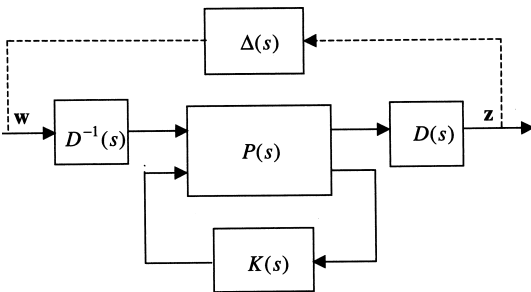

Fig. 4. Compensated Generalized Plant

plant disturbances $\mathbf{w}_d$, and weighted sensor noise $\mathbf{w}_\theta$. The objective variable **z** consists of stability variables associated with the plant uncertainty $\mathbf{z}_s$ and time-delay error z_τ, and performance variables associated with the pressure oscillations $\mathbf{z}_p$ and control-fuel injection z_u.

The generalized plant includes the following subsystems: the nominal plant model specified in state space realization, (A_p, G_1, G_2, C); shaping filters associated with plant disturbances and sensor noise, $W_d(s)$ and $W_\theta(s)$; performance weights associated with pressure oscillations and control-fuel injection, $W_p(s)$ and $W_u(s)$; and stability weight $W_\tau(s)$ associated with time delay errors. The plant uncertainty operator Δ_p and the phase uncertainty operator induced by the time delay errors Δ_τ are not included, since model uncertainties have been represented as uncertainty-induced disturbances, $\mathbf{w}_s$ and w_τ. The shaping filters, $W_d(s)$ and $W_\theta(s)$, are incorporated to characterize the frequency responses of the plant disturbances and sensor noises. The two performance weights, $W_p(s)$ and $W_u(s)$, are specified for the desired frequency response of acoustic motion and control-fuel injection to achieve a trade-off between the transient and steady-state responses.

Design of H_∞ Controller

The plant uncertainty operator Δ_p acts as an internal feedback, incorporating the effects of inaccuracies in the combustion dynamics model. The bound of Δ_p is specified in Eqs. (19) and (20). Based on the small-grain theorem [25, pp. 217–218], the necessary and sufficient condition of robust stability in the absence of plant disturbances (i.e. $\mathbf{d} = 0$), sensor noise (i.e., $\theta = 0$), and time-delay uncertainty (i.e., $w_\tau = 0$ or equivalently $\delta\tau = 0$) is:

$$\int_0^T \|\mathbf{z}_s\|^2 \, dt \leq \int_0^T \|\mathbf{w}_s\|^2 \, dt$$

$$\forall\, \mathbf{w}_s \in L_2[0, T]\, \forall\, T \in [0, \infty) \quad (21)$$

for the zero-state initial conditions with $\mathbf{z}_s \equiv \delta p \mathbf{x}_p$.

The parametric error of time delay $\delta\tau$ in modeling the distributed combustion of the injected secondary fuel induces an infinite-di-

mensional uncertainty, which is treated in the frequency domain. The non-rational transfer function $e^{-\delta\tau s}$ of time delay is treated as a multiplicative uncertainty:

$$\{(1 + \Delta_\tau(j\omega)W_\tau(j\omega):\|\Delta_\tau(j\omega)\| \leq 1\} \qquad (22)$$

where $\Delta_\tau(j\omega)$ accounts for the phase uncertainty and the magnitude of the perturbation is specified by the weight $W_\tau(j\omega)$. The normalized perturbation satisfies:

$$|e^{-\delta\tau j\omega} - 1| \leq |W_\tau(j\omega)| \; \forall \; \omega. \qquad (23)$$

where $\delta\tau \equiv \max_k |\tau_k|$. If only the effect of time-delay uncertainty is considered, with $\mathbf{d} = \boldsymbol{\theta} = \mathbf{w}_s = 0$, the necessary and sufficient condition of robust stability becomes:

$$\int_0^T \|z_\tau\|^2 \, dt \leq \int_0^T \|w_\tau\|^2 \, dt$$

$$\forall \, w_\tau \in L_2[0, T] \; \forall \; T \in [0, \infty) \qquad (24)$$

By eliminating the constraints of $w_\tau = 0$ and $\mathbf{w}_s = 0$ in Eqs. (21) and (24), respectively, a sufficient condition of robust stability is obtained as:

$$\int_0^T \{\|\mathbf{z}_s(t)\|^2 + \|z_\tau(t)\|^2\} \, dt$$

$$\leq \int_0^T \{\|\mathbf{w}_s(t)\|^2 + \|w_\tau(t)\|^2\} \, dt$$

$$\forall \begin{bmatrix} \mathbf{w}_s \\ w_\tau \end{bmatrix} \in L_2[0, T] \; \forall \; T \in [0, \infty) \qquad (25)$$

Remark 1: The constraints of zero plant disturbances (i.e., $\mathbf{d} = 0$) and zero sensor noise (i.e., $\theta = 0$) that are imposed in Eqs. (21) and (24) are still retained in Eq. (25).

Remark 2: By setting $w_\tau = 0$, Eq. (25) implies Eq. (21). Similarly, by setting $\mathbf{w}_s = 0$, Eq. (25) implies Eq. (24). Therefore, if Eq. (25) is satisfied, then the robust controller stabilizes the closed-loop systems for all perturbed plants within the uncertainty bounds of the modeled plant dynamics δp and time delay of secondary fuel combustion $\delta\tau$. This condition of robust

stability is not guaranteed to be satisfied by a simple combination of Eqs. (21) and (24).

The performance requirements signify a combination of reduction of acoustic energy, regulation of the control-fuel injection in the low frequency range, and rejection of plant disturbance and sensor noise. The ability to suppress longitudinal flow oscillations can be quantified by a positive quadratic energy-like function as follows:

$$H = \frac{1}{V} \int \int \int_V \left(\frac{p'(\mathbf{r}, t)}{\bar{p}}\right)^2 dV \qquad (26)$$

The controlled combustion chamber becomes free of acoustic oscillations as H approaches zero. Since the acoustic mode shapes are chosen to be orthonormal, Eq. (26) is simplified as:

$$H = \frac{1}{V} \left\langle \sum \varphi_n \eta_n, \sum \varphi_m \eta_m \right\rangle = \sum \eta_n^2 = \|\boldsymbol{\eta}\|^2 \qquad (27)$$

For each acoustic mode, the performance weight can be incorporated to specify the individual response. In this way, the performance variable $\mathbf{z}_p$ is defined by penalizing η using a frequency-dependent weight $W_p(s)$ as:

$$\hat{\mathbf{z}}_p(s) = W_p(s)\hat{\boldsymbol{\eta}}(s) \qquad (28)$$

and

$$W_p(s) = \begin{bmatrix} W_{p1}(s) & 0 & \cdots & 0 \\ 0 & W_{p2}(s) & \ddots & \vdots \\ \vdots & \ddots & \ddots & 0 \\ 0 & \cdots & 0 & W_{pN}(s) \end{bmatrix} \qquad (29)$$

where the Laplace transform of a time-dependent quantity is denoted by "^".

The acoustic pressure field is sometimes desired with a small steady error and a short settling time to improve efficiency. Thus, the procedure of selecting $W_p(s)$ is set as:

- The Bode magnitude plot of $W_{pi}(s)$ is a low-pass filter in the bandwidth range of interest corresponding to the natural frequency ω_i for a small steady oscillation.
- The shape of $W_{pi}(s)$ outside the bandwidth is assigned to be flat. The overshoot of $W_{pi}(s)$ determines the amplitudes of the mode shape. A trade-off between the transient and

steady-state responses results in a small set-tling time at the expense of large overshoot.

• The bandwidth range is altered by mean-flow-dependent model uncertainties. The nominal bandwidth corresponds to the natural frequency of acoustic oscillation. The bandwidth range for all perturbations is determined by the range of natural frequencies within the specified uncertainty bound.

The other performance requirements are related to the secondary-fuel injector that is used to distribute the control energy along the longitudinal direction of the combustion chamber. As the result of the inertial effects of fuel flow, the frequency response of the mass flow rate of control fuel is primarily designed to have a limited bandwidth and overshoot amplitude. A performance weighting function $W_u(s)$ is thus incorporated into the generalized plant model, and a new performance variable z_u is defined as:

$$\hat{z}_u(s) = W_u(s)\hat{u}(s) \tag{30}$$

where $\hat{u}(s)$ and $\hat{z}_u(s)$ are the Laplace transforms of $u(t) \equiv \dot{m}_{in}(t)$ and $z_u(t)$, respectively. The Bode magnitude plot of $W_u(s)$ determines the relevant bandwidth of control actions. A higher magnitude of $W_u(s)$ causes a smaller control effect that may often lead to a reduced overshoot of the pressure response. The shape of the $W_u(s)$ in the Bode magnitude plot outside the bandwidth range is assigned to be flat. However, the bandwidth range could be varied with model uncertainties. For example, the nominal bandwidth ranges from ω_1 to ω_N if N modes are considered. To determine the possible range of bandwidth for a variety of perturbations, the range of natural frequencies for the uncertainty bound needs to be identified.

The nominal performance is specified by a relationship between exogenous inputs, plant disturbance $\mathbf{d}$ and sensor noise $\boldsymbol{\theta}$, and performance variables, $\mathbf{z}_p$ and z_u. A shaping filter W_d is included in the generalized plant model to penalize the dominant frequency components of plant disturbances. The weighted plant disturbance $\mathbf{w}_d$ is used in performance specification, instead of $\mathbf{d}$ itself, as:

$$\hat{\mathbf{w}}_d(s) = W_d(s)\hat{\mathbf{d}}(s) \tag{31}$$

where $W_d(s)$ is a band-pass frequency-dependent function within the frequency range of the main components of $\mathbf{d}$. Similar conditions are used to penalize the sensor noise:

$$\hat{\mathbf{w}}_\theta(s) = W_\theta(s)\hat{\boldsymbol{\theta}}(s) \tag{32}$$

where $\hat{\mathbf{w}}_\theta$ is the weighted sensor noise and $W_\theta(s)$ is the shaping filter for the sensor noise $\boldsymbol{\theta}$.

An H_∞-optimal robust controller is designed such that the plant disturbances $\mathbf{d}$ and sensor noise $\boldsymbol{\theta}$ have minimum effects on acoustic motions and control actions from the energy perspective. In the absence of plant modeling uncertainties (i.e., $\mathbf{w}_s = 0$) and time delay uncertainties (i.e., $w_\tau = 0$), the nominal performance is specified as:

$$\int_0^T \{\|\mathbf{z}_P(t)\|^2 + \|\mathbf{z}_u(t)\|^2\}\, dt \leq \int_0^T \{\|\mathbf{w}_d(t)\|^2$$

$$+ \|\mathbf{w}_\theta(t)\|^2\}\, dt$$

$$\forall \begin{bmatrix} \mathbf{w}_d \\ w_\tau \end{bmatrix} \in L_2[0, T] \; \forall \, T \in [0, \infty) \tag{33}$$

If only initial conditions are considered (i.e., the covariance matrices of plant disturbance and sensor noise converge to zero), the H_∞ controller converges to an H_2 controller and the following cost functional is minimized:

$$J = \int_0^\infty \left(\frac{1}{V} \int\!\!\int\!\!\int_V \left(\frac{p'(\mathbf{r}, t)}{\bar{p}} \right)^2 dV + \|z_u\|^2 \right) dt \tag{34}$$

By eliminating the remaining constraints of $\mathbf{d} = 0$ and $\boldsymbol{\theta} = 0$ in Eq. (25) as well as the constraints of $\mathbf{w}_s = 0$ and $w_\tau = 0$ in Eq. (33), a sufficient condition of robust performance is obtained as:

$$\int_0^T \|\mathbf{z}\|^2\, dt \leq \int_0^T \|\mathbf{w}\|^2\, dt$$

$$\forall \, T \in [0, \infty) \; \forall \, \mathbf{w} \in L_2[0, T]$$

with $\mathbf{z}$

$$= \begin{bmatrix} \mathbf{z}_s \\ \mathbf{z}_p \\ z_u \\ z_\tau \end{bmatrix}; w = \begin{bmatrix} \mathbf{w}_s \\ \mathbf{w}_d \\ \mathbf{w}_\theta \\ w_\tau \end{bmatrix} \tag{35}$$

Remark 3: The robust performance condition in Eq. (35) is equivalent to simultaneously satisfying the conditions of robust stability and nominal performance that are individually satisfied in Eqs. (25) and (33), respectively. The robust performance condition in Eq. (35) may also be viewed as a consequence of the small gain theorem.

Remark 4: If Eq. (35) holds, then the robust controller (internally) stabilizes the closed loop control system for all plant perturbations with the desired performance, subject to the specified uncertainty bounds.

To facilitate the H_∞ robust control design, the generalized plant is expressed by a state-space realization through a series of transformations. First of all, every subsystem expressed by a transfer function is transformed into a state space realization in the time domain. The trans-

fer functions $W_p(s)$, $W_u(s)$, $W_\tau(s)$, $\mathbf{A}(s)$, $W_d(s)$ and $W_\theta(s)$ are expressed respectively as

$$\begin{cases} \dot{\mathbf{x}}_\eta = A_\eta \mathbf{x}_\eta + B_\eta \boldsymbol{\eta} \\ \mathbf{z}_p = C_\eta \mathbf{x}_\eta + D_\eta \boldsymbol{\eta} \end{cases} \begin{cases} \dot{\mathbf{x}}_u = A_u \mathbf{x}_u + B_u u \\ z_u = C_u \mathbf{x}_u + D_u u \end{cases}$$

$$\begin{cases} \dot{\mathbf{x}}_\tau = A_\tau \mathbf{x}_\tau + B_\tau u \\ z_\tau = C_\tau \mathbf{x}_\tau + D_\tau u \end{cases} \begin{cases} \dot{\mathbf{x}}_a = A_a \mathbf{x}_a + B_a(u + w_\tau) \\ \boldsymbol{\nu} = C_a \mathbf{x_a} + D_a(u + w_\tau) \end{cases}$$

$$\begin{cases} \dot{\mathbf{x}}_d = A_d \mathbf{x}_d + B_d \mathbf{w}_d \\ \mathbf{d} = C_d \mathbf{x}_d + D_d \mathbf{w}_d \end{cases}, \text{ and } \begin{cases} \dot{\mathbf{x}}_\theta = A_\theta \mathbf{x}_\theta + B_\theta \mathbf{w}_\theta \\ \theta = C_\theta \mathbf{x}_\theta + D_\theta \mathbf{w}_\theta \end{cases}.$$

$$(36)$$

Substitution of the above expressions into the corresponding equations and rearrangement of the results lead to the following state-space realization of the generalized plant, including the nominal plant, model uncertainties and performance specifications.

$$\begin{bmatrix} \dot{\mathbf{x}}_p \\ \dot{\mathbf{x}}_a \\ \dot{\mathbf{x}}_\eta \\ \dot{\mathbf{x}}_u \\ \dot{\mathbf{x}}_\tau \\ \dot{\mathbf{x}}_d \\ \dot{\mathbf{x}}_\theta \end{bmatrix} = \begin{bmatrix} A_p & G_1 C_a & 0 & 0 & 0 & G_2 C_d & 0 \\ 0 & A_a & 0 & 0 & 0 & 0 & 0 \\ [0\ B_\eta] & 0 & A_\eta & 0 & 0 & 0 & 0 \\ 0 & 0 & 0 & A_u & 0 & 0 & 0 \\ 0 & 0 & 0 & 0 & A_\tau & 0 & 0 \\ 0 & 0 & 0 & 0 & 0 & A_d & 0 \\ 0 & 0 & 0 & 0 & 0 & 0 & A_\theta \end{bmatrix} \begin{bmatrix} \mathbf{x}_p \\ \mathbf{x}_a \\ \mathbf{x}_\eta \\ \mathbf{x}_u \\ \mathbf{x}_\tau \\ \mathbf{x}_d \\ \mathbf{x}_\theta \end{bmatrix} + \begin{bmatrix} I & G_2 D_d & 0 & G_1 D_a \\ 0 & 0 & 0 & B_a \\ 0 & 0 & 0 & 0 \\ 0 & 0 & 0 & 0 \\ 0 & 0 & 0 & 0 \\ 0 & B_d & 0 & 0 \\ 0 & 0 & B_\theta & 0 \end{bmatrix} \begin{bmatrix} \mathbf{w}_s \\ \mathbf{w}_d \\ \mathbf{w}_\theta \\ w_\tau \end{bmatrix} + \begin{bmatrix} G_1 D_a \\ B_a \\ 0 \\ B_u \\ B_\tau \\ 0 \\ 0 \end{bmatrix} u$$

$$(37)$$

$$\begin{bmatrix} \mathbf{z}_s \\ \mathbf{z}_p \\ z_u \\ z_\tau \end{bmatrix} = \begin{bmatrix} \delta p & 0 & 0 & 0 & 0 & 0 & 0 \\ [0\ D_\eta] & 0 & C_\eta & 0 & 0 & 0 & 0 \\ 0 & 0 & 0 & C_u & 0 & 0 & 0 \\ 0 & 0 & 0 & 0 & C_\tau & 0 & 0 \end{bmatrix} \begin{bmatrix} \mathbf{x}_p \\ \mathbf{x}_a \\ \mathbf{x}_\eta \\ \mathbf{x}_u \\ \mathbf{x}_\tau \\ \mathbf{x}_d \\ \mathbf{x}_\theta \end{bmatrix} + \begin{bmatrix} 0 \\ 0 \\ D_u \\ D_\tau \end{bmatrix} u$$

$$(38)$$

$$\mathbf{y} = [C\ \ 0\ \ 0\ \ 0\ \ 0\ \ 0\ \ C_\theta] \begin{bmatrix} \mathbf{x}_p \\ \mathbf{x}_a \\ \mathbf{x}_\eta \\ \mathbf{x}_u \\ \mathbf{x}_\tau \\ \mathbf{x}_d \\ \mathbf{x}_\theta \end{bmatrix}$$

$$+ [0\ \ 0\ \ D_\theta\ \ 0] \begin{bmatrix} \mathbf{w}_s \\ \mathbf{w}_d \\ \mathbf{w}_\theta \\ w_\tau \end{bmatrix} \qquad (39)$$

The generalized plant model is an ensemble of Eqs. (37) through (39), as delineated below.

$$P(s) \Leftrightarrow \begin{cases} \dot{\mathbf{x}} = A\mathbf{x} + B_1 \mathbf{w} + B_2 u \\ \mathbf{z} = C_1 \mathbf{x} + D_{12} u \\ \mathbf{y} = C_2 \mathbf{x} + D_{21} \mathbf{w} \end{cases} \qquad (40)$$

The states of the generalized plant consist of those of the nominal plant and actuator dynamics, along with their model uncertainties, and performance requirements specified by weighting functions and shaping filters. Note that the order of the generalized plant model $P(s)$ in Eq.

(40) can be reduced by means of the Hankel operator [25].

The generalized plant model $P(s)$ suffers from the conservative condition for performance specifications in Eq. (35). An attempt is, therefore, made to improve the controller performance by the D-K iteration procedure [14], in which the generalized plant model $P(s)$ is compensated as $D^{-1}(s)P(s)D(s)$ with $D(s)$ having the following property:

$$D(s)\Delta(s) = \Delta(s)D(s) \qquad (41)$$

Note that the block matrix $\Delta(s)$ in Fig. 4 includes both model uncertainties and performance requirements. The controller design can take advantage of available software tools, such as the linear matrix inequalities (LMI) toolbox [26].

PARAMETRIC STUDY AND SIMULATION RESULTS

To study the characteristics of the controller, we consider herein as a specific example a nominal plant model involving the first four modes of longitudinal pressure oscillation. The natural frequency (in radians) of the fundamental mode, normalized with respect to $\pi\bar{a}/L$, is taken to be unity. The linear parameters D_{ni} and E_{ni} in the nominal model, Eq. (12), as well as the spatial distribution b_k and time delay τ_k of the distributed combustion source, are taken from Fung *et al.* [1], representing a typical situation encountered in several practical combustion chambers. An integrated research project comprising laser-based experimental diagnostics and comprehensive numerical simulation is currently being conducted to provide direct insight into the combustion dynamics in a laboratory dump combustor [27]. Included as part of the results are the system and actuator parameters under feedback actions, which can be directly incorporated into the robust controller design established in the present work.

Based on the discussion in Section 3, the performance weights $W_p(s)$ and $W_u(s)$ associated with the chamber pressure oscillations and the control-fuel injection, respectively, and the shaping filters $W_d(s)$ and $W_\theta(s)$ associated with
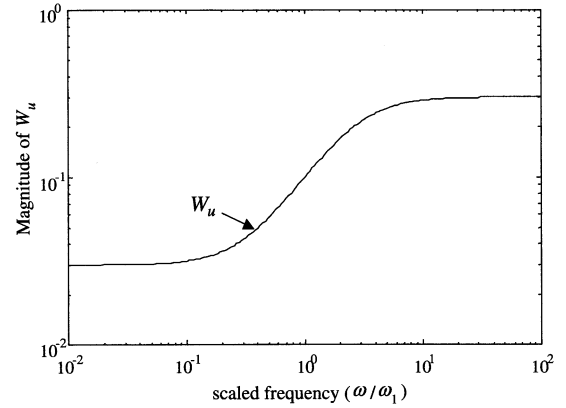

Fig. 5. Performance Weighting Associated with Control-Fuel Injection.

the plant disturbance and sensor noise, respectively, are chosen as:

$$[W_p \; W_u \; W_d \; W_\theta] \equiv \left[qI \;\; \frac{r(10s + 8)}{s + 5} \;\; I \;\; I \right] \qquad (42)$$

where q and r are positive scalars, representing the weights of acoustic motion and control action, respectively. A more stringent requirement for rejecting plant disturbances (or sensor noise) is specified by increasing q (or r). If q is set large relative to r, the response of acoustic motion is more emphasized than the control action, and vice versa. The shape of the performance weighting associated with control-fuel injection, $W_u(j\omega)$, in the frequency domain is shown in Fig. 5, where the natural frequencies of the first four modes fall into the bandwidth of [0.8, 5.0], taking into account frequency uncertainties. W_u acts as a derivative operator for regulating the transient response of control-fuel injection within the specified bandwidth. Its shape is assigned to be flat outside the bandwidth to accommodate the steady response. The shaping filters $W_d(s)$ and $W_\theta(s)$ are chosen as constant identity matrices, because the process and measurement disturbances are considered to be white noise. The stability weighting associated with the time delay errors of control-fuel injection, $W_\tau(s)$, is determined by Eq. (23), and its magnitude in the frequency domain is shown in Fig. 6. According to Eq. (23), $W_\tau(j\omega)$ is chosen to cover the envelope $e^{\delta\tau j\omega} - 1$. Its first-order approximation is used in the present simulation study.
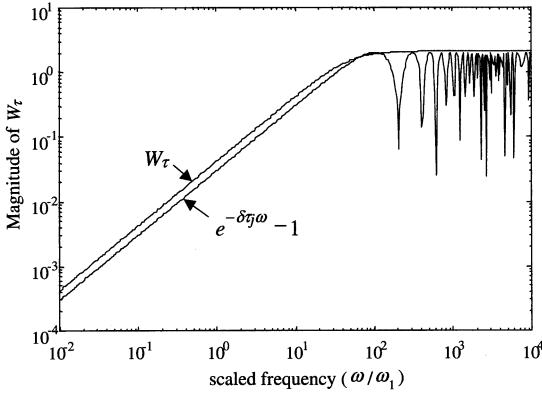
Fig. 6. Stability Weighting Associated with Time Delay Errors

TABLE 2

Simulation Parameters for Nominal Case

Time-delay error	$\delta\tau = 0.3$
Weighting factors	$q = 0.1; r = 0.1$
Intensity of white plant disturbance	10^{-3}
Intensity of white sensor noise	10^{-3}

A series of simulation experiments have been conducted to investigate the effect of the various weights associated with pressure oscillation (q) and control-fuel injection (r) on the robustness and performance of the control system. Also included in the parametric investigation are the bound δp of plant model uncertainties and the maximum time delay $\delta\tau$ of the distributed combustion of control-fuel. Figure 7 exhibits the relationship among the parameters δp, q and r. The uncertainty bound of combustion time delay $\delta\tau$ is set to be 0.3. The ratio of q to r specifies the trade-off between the response of acoustic motions and the bandwidth capability of the fuel injector, and the ratio of δp to q or r the trade-off between the robustness and performance of the closed-loop system. The values of q and r jointly determine the ability to reject
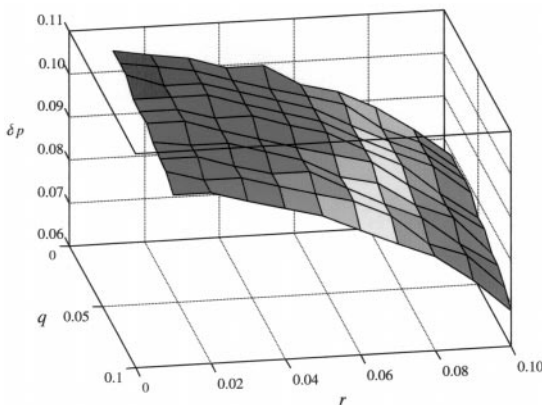
exogenous inputs (i.e., plant disturbance and sensor noise), and increasing r implies that the transient response of the closed-loop system is more emphasized. For a given uncertainty bound, the desired performance can be determined based on the plot in Fig. 7. On the other hand, for a specified performance of the control system, the corresponding plant modeling uncertainty bound may not fully guarantee stability, because Eq. (35) represents a sufficient, not necessary, condition for robust performance. The maximum value of the model uncertainty bound is found to be 0.11.

The time responses of pressure oscillation and control-fuel injection rate are studied for two cases: one for the nominal system and the other for a perturbed system with 50% parameter errors relative to their nominal values. The simulation parameters are given in Table II. Figure 8 shows the time history of pressure oscillation at the chamber head end for each mode in the nominal case that is set as a benchmark for evaluating the efficacy of the robust controller under induced disturbances. The controller is activated to suppress unsteady
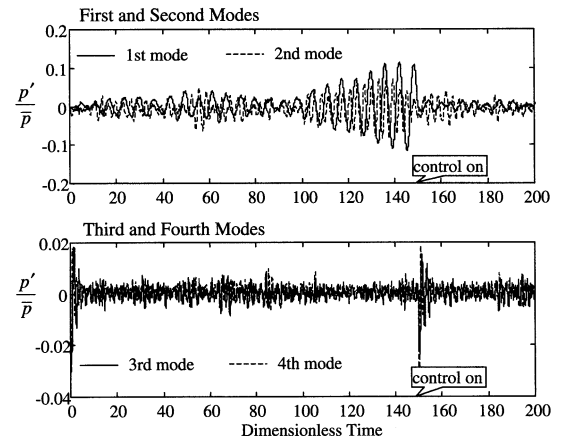

Fig. 7. Relationship between Plant Uncertainty and Performance; $\delta\tau = 0.3$.

Fig. 8. Time History of Pressure Oscillation in Nominal Case.
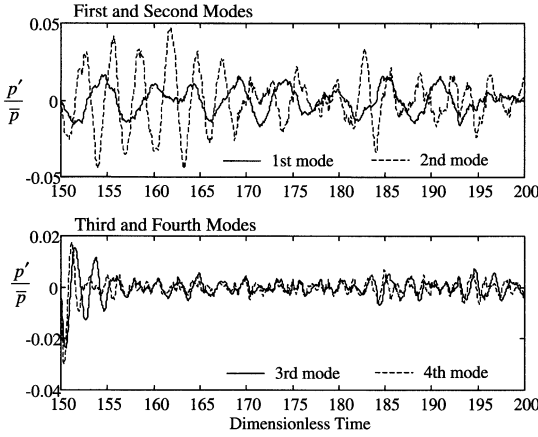
Fig. 9. Time History of Pressure Oscillation in Nominal Case under Feedback Control.

Fig. 11. Time History of Acoustic Energy and Control Fuel Injection Rate in Perturbed System with 50% Parametric Uncertainty.

motions when the amplitude of the sensor output reaches a preset threshold value. The closed-loop system is asymptotically stable without any exogenous input, and the controller eliminates undesired pressure oscillations within a short period. With plant disturbances and sensor noise, the robust feedback controller reduces the oscillation of the first two modes to an acceptable level in a short setting time, without increasing the amplitude of the last two modes. The system response is significantly improved by the feedback control. Figure 9 shows the close-up view in the period after the controller is activated. The pressure oscillation is reduced to about 1% of the mean pressure.
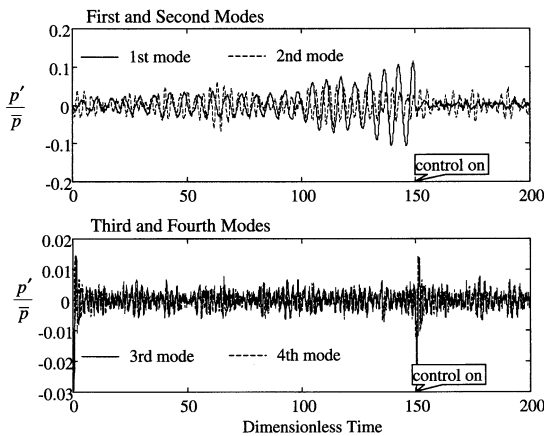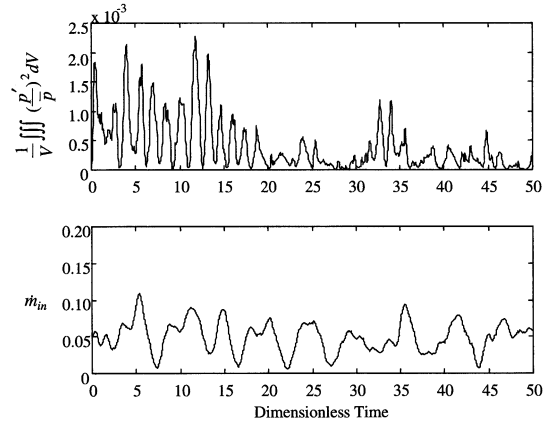
Figure 10 shows the time response of the

perturbed system with 50% parametric uncertainties. In comparison with the nominal case shown in Fig. 8, the control system guarantees robust performance for a wide variety of perturbed plants within specified uncertainties. The similarity between the responses in the nominal and perturbed cases reveals the robust characteristics of the H_∞ controller. One of the major issues in the design of an active combustion controller is the energy required to suppress unsteady motions as opposed to the mechanical energy of the oscillatory flow. To explore this point, the energy of acoustic motion and the injected rate of control fuel are also calculated, giving the result shown in Fig. 11, where the injection rate of control-fuel $\dot{m}_{in}$ has been scaled by $-\bar{R}\Delta H_c/\omega_1^2 \bar{C}_v \bar{p}_0$ to make it nondimensional.

The impact of the time-delay uncertainty $\delta\tau$ on the closed-loop system response is presented in Fig. 12, showing the pressure oscillations at the chamber head end for $\delta\tau = 0.6$, 1.2, 1.6 and 2.2. The other parameters remain identical to those of the nominal case. If the actuator model is made perfect (i.e. $\delta\tau = 0$), the combustion control system becomes robustly stable for the plant uncertainty bound $\delta p = 0.16$. The distributed actuator for secondary fuel injection must be designed not to exceed a specified limit of the time delay bound. Obviously, the disturbance rejection capability of the controller diminishes with an increase in $\delta\tau$, and the closed-loop system becomes unstable as $\delta\tau$ is made

Fig. 10. Time History of Pressure Oscillation in Perturbed System with 50% Parametric Uncertainty.
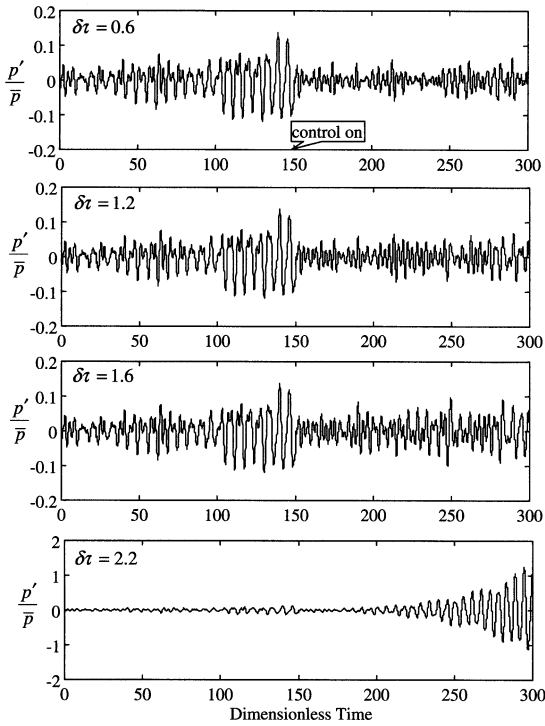
Fig. 12. Time Histories of Pressure Oscillation in Nominal Cases with Various Combustion Time-Delay Uncertainties.

large enough. The present design exhibits nominal stability of the control system for a maximum value of $\delta\tau$ around 2.

Actuator saturation is one of the critical issues in robust controller design, especially for the H_∞-based controller design. Figure 13 shows the pressure oscillation at the chamber head end for the nominal case when the secondary-fuel actuator could be saturated. The upper and
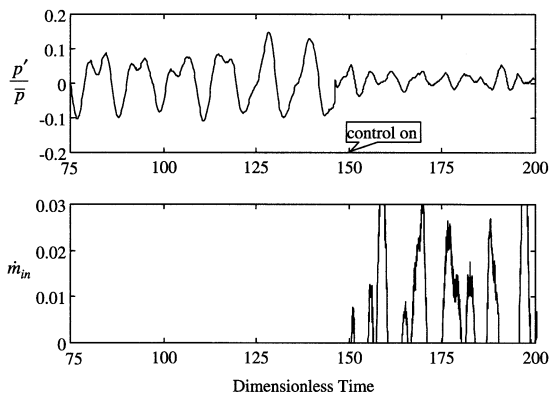

Fig. 13. Closed-Loop System Response of Nominal Case with Actuator Saturation.

lower limits of saturation are set as 0.03 and 0.0, respectively. The closed-loop system under actuator saturation still exhibits high performance, due to the proper choice of the control weight $W_u(s)$.

SUMMARY AND CONCLUSIONS

A comprehensive framework has been established for robust feedback control of longitudinal combustion dynamics in propulsion systems. The control action is executed by injecting auxiliary liquid fuel, and is modeled as a distribution of time-delayed combustion sources. The controller design methodology is based on the H_∞-based structured singular value (μ) algorithm for disturbance rejection, and takes into consideration the effects of unmodeled dynamics, parametric errors, and sensor noise. A physically intuitive approach is presented for selection of frequency-dependent weights for controller synthesis and analysis where very few, if any, iterations are needed to arrive at the final design. The global behavior of the weighting functions is represented by a time-domain description of performance specifications. The results of the parametric study provide flexibility for selection of stability and performance margins in the controller design. Simulation experiments show that the controller is not only capable of suppressing pressure oscillations in a typical combustion chamber within a short period of time, but also retains robust stability and performance under exogenous disturbances and parametric uncertainties.

REFERENCES

1. Fung, Y. T., Yang, V., and Sinha, A., *Comb. Sci. Technol.*, 78:217–245 (1991).
2. McManus, K. R., Poinsot, T. and Candel, S. M., *Prog. Energy Comb. Sci.*, 19:1–29 (1993).
3. Schadow, K. C., Yang, V., Culick, F. E. C., Rosfjord, T. J., Sturgess, G. J., and Zinn, B. T., *Active Combustion Control for Propulsion Systems*, Report No. AGARD-R-820, 1997.

4. Fung, Y. T., and Yang, V., *J. Propulsion and Power*, 8:1282–1289 (1992).

5. Yang, V., Sinha, A., and Fung, Y. T., *J. Propulsion and Power*, 8:66–73 (1992).

6. Neumeier, Y., and Zinn, B. T., *Twenty-Sixth Symposium (International) on Combustion*, The Combustion Institute, 1996, p. 2811–2818.

7. Bloxsidge, G. J., Dowling, A. P., Hooper, N., and Langhorne, P. J., *J. Theoretical and Applied Mechanics*, 6:317–325 (1987).

8. Langhorne, P. J., Dowling A. P., and Hopper N., *J. Propulsion and Power*, 6:324–333 (1990).

9. Schadow, K. C., Gutmark, E., and Wilson, K. J., *Comb. Sci. Technol.*, 81:285–300 (1992).

10. Gulati, A., and Mani, R., *J. Propulsion and Power*, 8:356–377 (1992).

11. Annaswamy A. M., and Ghoniem, A. F., *IEEE Control Systems Magazine*, 15:49–63 (1995).

12. Hantschk, C., Hermann, J., and Vortmeyer, D., *Twenty-Sixth Symposium (International) on Combustion*, The Combustion Institute, 1996, p. 2835–2841.

13. Doyle, J. C., Glover, K., Pramod, P., and Francis, B. A., *IEEE Trans. on Auto. Cont.*, 34:831–847 (1989).

14. Packard, A., and Doyle, J. C., *Automatica*, 29:71–109 (1993).

15. Packard, A. and Doyle, J. C., *Trans. of the ASME*, 115:426–438 (1993).

16. Safonov, M. G., Athans, M., *IEEE Trans. on Auto. Cont.*, 22:1237–1254 (1977).

17. Doyle, J. C., *IEEE Trans. an Auto. Cont.*, 23:756–757 (1978).

18. Billoud, G., Galland, M. A., Huynh C., and Candel, S., *Comb. Sci. Technol.*, 81:257–283 (1992).

19. Allen, M. G., Butler, C. T., Johnson, S. A., Lo, E. Y., and Russo. F, *Comb. Flame*, 94:205–214 (1993).

20. Kemal, A, and Bowman, C. T., *Twenty-Sixth Symposium (International) on Combustion*, The. Combustion Institute, 1996, p. 2803–2809.

21. Koshigoe, S., Komatsuzaki, T., and Yang, V., *J. of Propulsion and Power*, 15:383–389 (1999).

22. Menon, S. and Sun, Y, *32nd AIAA/ASME/ASEE/SAE Joint Propulsion Conference*, Buena Vista, Florida, 1996 July 1–3, AIAA Paper 96-2759.

23. Fung, Y. T., *Active Control of Linear and Nonlinear Pressure Oscillations in Combustion Chambers*, PhD thesis, The Pennsylvania State University, 1991.

24. Culick, F. E. C.. *Acta Astronautica*, 3:715–756 (1976).

25. Zhou, K., Doyle, J. C., and Clover K., *Robust and Optimal Control*, Prentice-Hall, New Jersey, 1996.

26. Gahinet, P., Nemirovski, A., Laub, A. J., and Chilali, M., *LMI Control Toolbox for Use with MATLAB*, The Math Works Inc., Natick, MA, 1994.

27. Yang, V., Santavicca, D. A., and Ray, A., Intelligent Control of Gas Turbine Combustion Dynamics for Performance and Emission Improvement, In *Proceedings of Eleventh Propulsion Meeting*, US Office of Naval Research, Arlington, VA, 1998, p. 52–58.

28. Krstic, M., Krupadanam, A., and Jacobson, C., "Self-Tuning Control of a Nonlinear Model of Combustion Instabilities," Submitted to *IEEE Trans. on Control Systems Technology*, 1997.